Proceedings of 8th International Conference on Short and Medium Span Bridges

Niagara Falls, Canada 2010

NON-LINEAR ANALYSIS OF MULTI-HAZARD PERFORMANCE OF CYLINDRICAL CONCRETE FILLED STEEL TUBES BRIDGE PIERS

Pierre Fouché
Department of Civil, Structural, and Environmental Engineering, University at Buffalo, USA

Michel Bruneau
Department of Civil, Structural, and Environmental Engineering, University at Buffalo, USA

ABSTRACT

Advanced finite element techniques are used to investigate the multi-hazard (earthquake and blast) performance of Concrete-Filled Steel Tubes (CFSTs) and Concrete Filled Double Skinned Tubes (CFDSTs) for bridge engineering applications. Specimens of both sections are analyzed using the finite element package LS-DYNA under similar seismic and blast loading. First, behavior of CFSTs recorded in seismic and blast tests are reproduced using the finite element program and compared to experimental results for accuracy and adequacy, then the techniques developed for this analysis are carried over to the modeling and analysis of CFDSTs. LS-DYNA captured generally well the behavior of CFSTs in both hazards, particularly the non-cyclic inelastic behavior under blast loads. Although the techniques used for the seismic analysis can be refined, the main features established experimentally are present. Also it is proven here that CFDSTs can develop their full strength over longer yield plateau than their CFSTs counterparts. Together, these two composite systems constitute valuable alternatives to conventional column piers of bridges that need be designed for multiple hazards.

1. INTRODUCTION

This paper investigates the effectiveness of advanced finite element to replicate and predict the multi-hazard performance of Concrete Filled Steel Tube (CFST) and Concrete Filled Double Skinned Tube (CFDST) sections used as bridge piers. The primary focus is on seismic cyclic inelastic resistance and performance in close range blast loading as anticipated in a terrorist attack. This focus on multi-hazard performance is motivated by the emerging philosophy in bridge engineering that favors cost-effective systems that can provide sufficient performance against each hazard for bridges erected in environments where they can be exposed to multiple hazards.

The finite element package LS-DYNA is used to carry out this multi-hazard analysis. This paper presents a brief overview of the CFDST concept, followed by the results of analyses conducted to reproduce the experimental behavior obtained for CFSTs under loadings similar to what can occur in earthquake and blast hazards respectively (Marson and Bruneau 2000; Fujikura and Bruneau 2007). This step is necessary to verify and validate the LS-DYNA models used to carry the complex inelastic analysis this entails. Following that step, CFDST sections with various diameter-to-thickness ratios and having approximately the same areas of steel and concrete as the cross-sections used in those previous studies are modeled in LS-DYNA to assess their performance in that bi-hazard framework.

2. THE CONCRETE FILLED DOUBLE SKINNED TUBE CONCEPT

CFDST is a kind of steel-concrete-steel "sandwich" section formed by two concentric steel tubes separated by a concrete filler as shown on Figure 1. That configuration seeks to draw upon the benefits in strength, toughness and stiffness derived for steel-sandwich construction by placing the steel at the periphery of a filler material (as described, for example, in Montague 1975). Due to the cylindrical shape of this sandwich construction, a void normally exists in the center of a CFDST section; this allows the resulting cross section to concentrate materials where needed for optimal performance. Also, because of the obvious similarities with concrete-filled tubes (CFSTs), the concrete core is expected to be confined by the tubes which should provide, in return, support to the tubes against local buckling. That synergy between the tubes and the core in resisting load is expected to result in a section with good structural and energy dissipation qualities compared to, say, having uniquely the tubes working in unison.

CFDSTs have been previously studied by some researchers for their strengths under axial and bending loads (Shakir-Khalil 1991) and for prospective applications in the petroleum industry to cope with the local and global stability concerns which often prevent components of oil platform made of hollow steel tubes from developing their full yielding strength (API 1989; Wei et Al. 1995). Others have attempted to characterize their potential to dissipate energy under cyclic loading (Tsai et al. 2001, Tao et al. 2003); nevertheless little is known about their worthiness for blast applications.

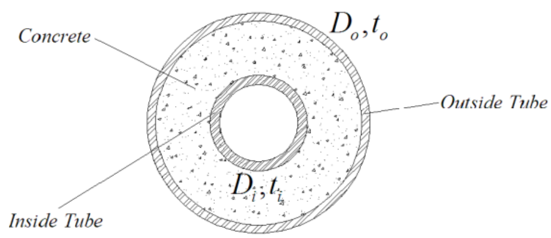

Figure 1. Concrete filled double skin tube section

3. PARAMETERS FOR FINITE ELEMENT ANALYSIS OF CFSTS AND CFDSTS

3.1 Specimens Selection

The CFST specimens selected for this analysis are found in the works by Marson and Bruneau and Fujikura and Bruneau mentioned earlier. The former tested four specimens of concrete-filled tubes with various diameters (D), thickness (t), steel and concrete strengths (f_y and $f_c^{'}$) but with constant height (H) under cyclic displacement combined to various levels of axial loads (P). The later conducted blast experiments on ten quarter scale models of concrete-filled tube pier-columns with various charge weights (W) at variable heights (Z) and scaled distances ($X/W^{1/3}$) with respect to the specimens. Tables 1 and 2 below show some of the specimens studied by those authors and their respective characteristics and loadings. In Tables 1 and 2, the scaled distances are expressed as multiples of the smallest scaled distance *x* considered in this paper.

Table 1: CFSTs tested by Marson and Bruneau (2000)

CFST	H (mm)	D (mm)	t (mm)	$f_c^{'}$ (MPa)	f_y (MPa)	P (kN)
64	2200	406.4	5.5	37	442	1000
34	2200	323.9	7.5	40	415	1920
42	2200	406.4	9.5	35	505	1920
51	2200	323.9	5.5	35	405	1600

The finite element study described in this paper concerns only specimen CFST 64 and tests 5, 7 and 10 showed on Tables 1 and 2 because they permit to cover adequately the range of inelastic behavior observed during those experimental works.

Table 2: Specimens tested by Fujikura and Bruneau (2007)

TESTS	H (mm)	D (mm)	t (mm)	$f_c^{'}$ (MPa)	f_y (MPa)	Z (mm)	$X/W^{1/3}$ ($m/kg^{1/3}$)
5	1500	127.0	3.0	43.4	254	750	2.27 *x*
7	1500	101.6	3.1	43.2	357	250	1.00 *x*
10	1500	127.0	2.8	43.4	254	250	1.43 *x*

The CFDST specimens are derived from the CFSTs selected earlier in such a way that they use approximately the same amount of material resulting in section with nearly identical cost. Their void ratio (χ) and their compactness ratios (D_o/t_o and D_i/t_i) are varied so as to cover a wide range of possible combinations. Tables 3 and 4 below show the different CFDST components obtained in that fashion for the two types of analysis performed. For the CFDST specimens the numbers in the first column of those tables represent in that order the depth-to-thickness ratios for the inside and outside tubes and the void ratio which is defined as the ratio of the radius of the inner tube to the radius of the outer tube which is an indirect measure of the amount of concrete used in the section. To reduce the scope of the analysis in this paper, only the loading from tests 5 and 10 are considered for blast analysis of the CFDSTs.

Table 3: CFDSTs derived for pushover and cyclic analysis

CFDST	H (mm)	D_i (mm)	D_o (mm)	t_i (mm)	t_o (mm)	$f_c^{'}$ (MPa)	f_y (MPa)
9_132_24	2200	101.6	419.1	11.11	3.18	37	442
16_88_24	2200	101.6	419.1	6.35	4.76	37	442
64_88_24	2200	101.6	419.1	1.59	4.76	37	442
110_184_60	2200	302.5	506.0	2.75	2.75	37	442
166_113_50	2200	228.6	463.6	1.38	4.13	37	442

Table 4: CFDSTs derived for blast analysis

CFDST	TESTS	H (mm)	D_i (mm)	D_o (mm)	t_i (mm)	t_o (mm)	$f_c^{'}$ (MPa)	f_y (MPa)
16_88_36	5	1500	50.8	139.7	3.18	1.59	43.4	254
16_88_36	10	1500	50.8	139.7	3.18	1.59	43.4	254

3.2 Finite Element Package

Because of the highly non-linear behaviors anticipated in analyzing CFSTs and CFDSTs in this bi-hazard framework, the advanced finite element analysis package LS-DYNA is chosen as an analysis tool. Both the implicit and the explicit solvers in LS-DYNA are used. The implicit solver in LS-DYNA is an incremental-iterative numerical algorithm based on Newton and quasi-Newton methods of analysis and is adapted to solve both linear and non-linear static, quasi-static and dynamic problems with low frequency content that may involve contact, strain rate and material and geometric non-linearities. For implicit dynamic analysis, the Newmark method is used for integration of the equation of motion. The characteristics of this solver are well discussed elsewhere (LSTC 2007). The implicit solver was selected to carry-out cyclic pushover analysis of the sections studied and replicate and predict the behaviors of CFSTs and CFDSTs under seismic loading. On the other hand, the explicit solver in LS-DYNA which is built around the central difference scheme is adopted to solve the equation of motion that describes the transient problem in the blast analysis. This solver is mostly suited to situations involving high frequency short duration impulsive loading, high strain-rate, contact and geometric and material non-linearities (LSTC 2007) which are all present in this study. LS-DYNA also offers the unique feature of coupling implicit and explicit analysis in any order that fits the problem to be solved (for an application see Rust and Schweizerhof 2003).

3.3 Geometry

To model the steel tubes in both CFSTs and CFDSTs, fully integrated 4-noded shell elements are used whereas 8-noded tetrahedron solid elements with reduced integration and hourglass control for the concrete core are deemed appropriate to capture with sufficient accuracy the behavior of the core under blast load. In cyclic loading, it has been found that better accuracy is achieved by using fully integrated solid elements; however, this induces a penalty in term of computation time. Figure 2 below shows screenshots of the CFST models.

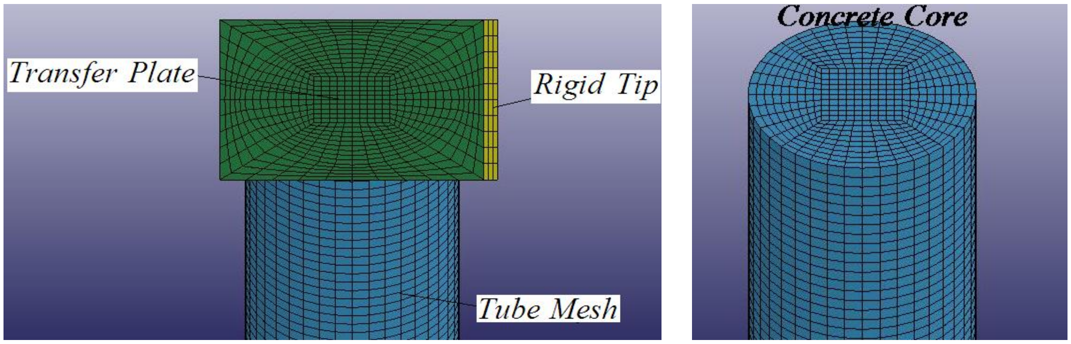

Figure 2. Details of the CFST models

3.4 Material Constitutive Models

For the CFSTs, the steel stress-strain curves are available from the experiments by Fujikura and Bruneau; however partial curves only are available from the study by Marson and Bruneau. When the full curves are available they are directly input in the material model considered for the steel, for the partial curves it is assumed that the yield stress is maintained until failure. Two Von-Mises based plasticity material models respectively coded in LS-DYNA as Material 24 (LSTC 2007) and Material 153 (Huang and Mahin 2008) are used to model the steel tube. In material 24, damage is considered intrinsically using ultimate strain as failure criterion. On the other hand Material 153 was developed specifically to reproduce low-cycle fatigue as observed in steel material. Both models can capture strain hardening effects if desired. In material 24, strain rate effect is accounted for using the Cowper-Symonds model which scales the yield stress by a factor which varies with the actual strain rate (LSTC 2007). Material 153 does not consider strain rate effects since it was not developed for that purpose. Thus, Material 24 is used for unidirectional pushover analysis or blast analysis in which failure is likely to be attained when the composite section reach an ultimate deformation limit state whereas Material 153 is judged more adapted to the cyclic analysis in which failure is due to low-cycle fatigue.

For the concrete core, the model opted for was Mat72 REL3 in LS-DYNA whose formulation is based upon the William-Warnke three-invariant plasticity concrete material model (Malvar and Simons 1996). This model uses three shear failure surfaces to represent the behavior of the concrete material. It can account not only for confinement of the core, but also for strain-rate effects via a tabulated-function derived from experimental data. The model considers both shear and volumetric damage in the concrete. However, an erosion algorithm available in LS-DYNA has to be appended to the concrete model as an option to physically display damage.

3.5 Considerations of Bond and Friction

For CFSTs, no slip was visible afterwards at the interface between the steel tube and the concrete core in the experimental works reported. It can be assumed that perfect bond exists between the tube and the core. Thus, in the CFST models corresponding nodes on the contact surface between the steel tube and the concrete core are simply constrained to each other.

3.6 Boundary Conditions, Imperfections and Damping Considerations

Fully fixed conditions are assumed to allow progressive hinging at the fixed ends of the specimens. Although the tubes were embedded in composite foundations in both sets of experiments mentioned, no embedment length is considered in the LS-DYNA models under seismic and blast loading

Geometric imperfections are introduced into the models for pushover and cyclic analysis. They are, however, deemed of little influence over the response of the components under blast loads. Although other methods exist, geometric imperfections are introduced in this paper by specifying a harmonic perturbation to a portion of the model (Rust and Schweizerhof 2003).

Damping is considered only for blast analysis. A global value of 1% is added to the model solely to make sure that models that have reached their maximum deformation without completely fracturing can return to a deformed equilibrium position in the free vibration phase that follows the attainment of maximum deformation.

3.7 Loading

3.7.1 Pushover and Cyclic Analysis

For pushover and cyclic analysis a plate whose meshes coincide with the meshes of the tubes and the concrete core is used as a transfer element at the top of each specimen. The plate is terminated by a rigid tip to which the displacement history is applied for pushover and cyclic analysis as shown in Figure 2 above. Pushover and cyclic analysis are done using a displacement control approach. For the pushover analysis a constant velocity is applied at the rigid tip whereas for the cyclic analysis a modified displacement history- based on the ATC-24 protocol-provides the loading. For all inelastic excursions in this displacement history only two full cycles are considered compared to the three cycles considered for inelastic excursions up to 3% percent drift in ATC-24.

3.7.2 Blast

Blast overpressures are applied to the models using the airblast function in LS-DYNA which is an implementation of the airblast pressure data available in ConWep, a collection of conventional weapons effects calculations from the equations and curves of the US Army technical manual TM 5-855-1. In the version of LS-DYNA used, reflection of blast wave is not included in the computation of the peak overpressure and impulse. As a consequence a factor is applied to the resulting pressure history so that the resulting peak impulse matched the peak reflected impulse predicted for the tests using the blast overpressure generation program BEL and the correction method presented by Fujikura and Bruneau to account for the reduction in impulse due do the roundness of the section.

4. MULTIHAZARD FINITE ELEMENT ANALYSIS RESULTS OF CONCRETE-FILLED TUBE

LS-DYNA implicit is the solver chosen for the cyclic analysis of CFST64. Besides mesh refinement, displacement and energy tolerances of 1% are imposed for adequate convergence. Those tolerances could be lower but the significant increase in computation time recorded would not justify the marginal improvement in accuracy that would result. The cyclic pushover result for CFST64 in LS-DYNA is shown in Figure 3 below.

The ranges for strength and drift are well captured. However the pinching in the hysteresis loops observed during the test is not well reproduced. This pinching is influenced by the progressive buckling of the steel tube and the crushing in the compression zone of the concrete core. This inaccuracy might be traced back to the fact that the finite element model was not a faithful reproduction of the entire experiment, notably, as mentioned earlier, to reduce computation time the full displacement history of the test is not applied. This might explain why the pinching in the model is further delayed as the number of inelastic cycles necessary to take the specimen close to its fatigue limit was not applied.

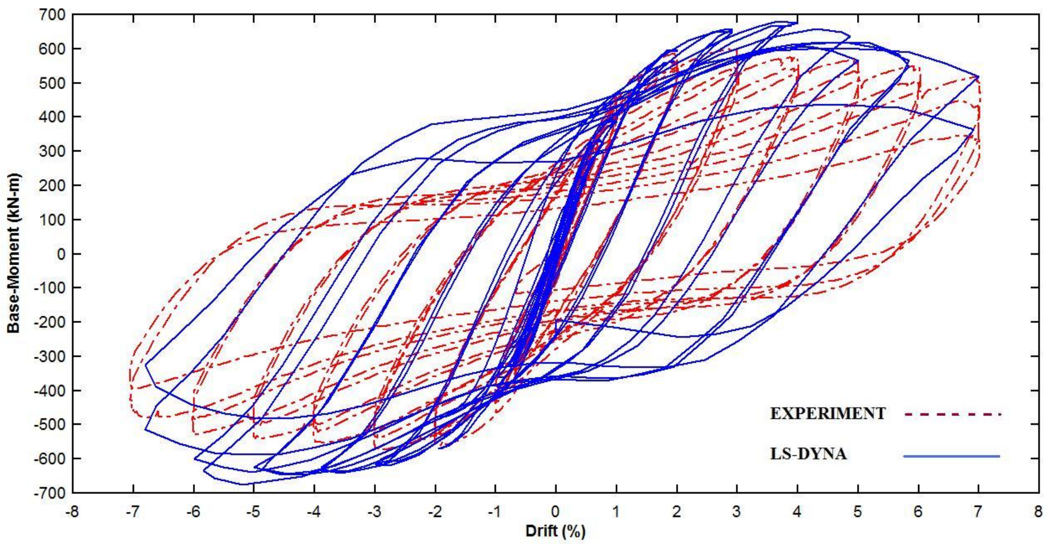

Figure 3. Cyclic pushover results for CFST64

After mesh refinement the blast analysis using the explicit solver in LS-DYNA converged with adequate accuracy and captured exactly the ductile sequence of limit states (yielding-plastification-fracture) experimentally observed under blast loading. Figures 4 a and b respectively show plastic deformation as measured in Test 5 and test 10. In particular, the angles of rotation from the finite element model match the ones measured after the tests. The displacement fields match also the ones measured in the tests (Figure 8). In test 10 the partial fracture of the shell and the concrete core is well captured.

In Figure 5, the finite element model captured the fracture observed for the specimen of test 7. It can be seen that the bottom part of the specimen blows away as seen in the test while the columns fracture at its top and its base.

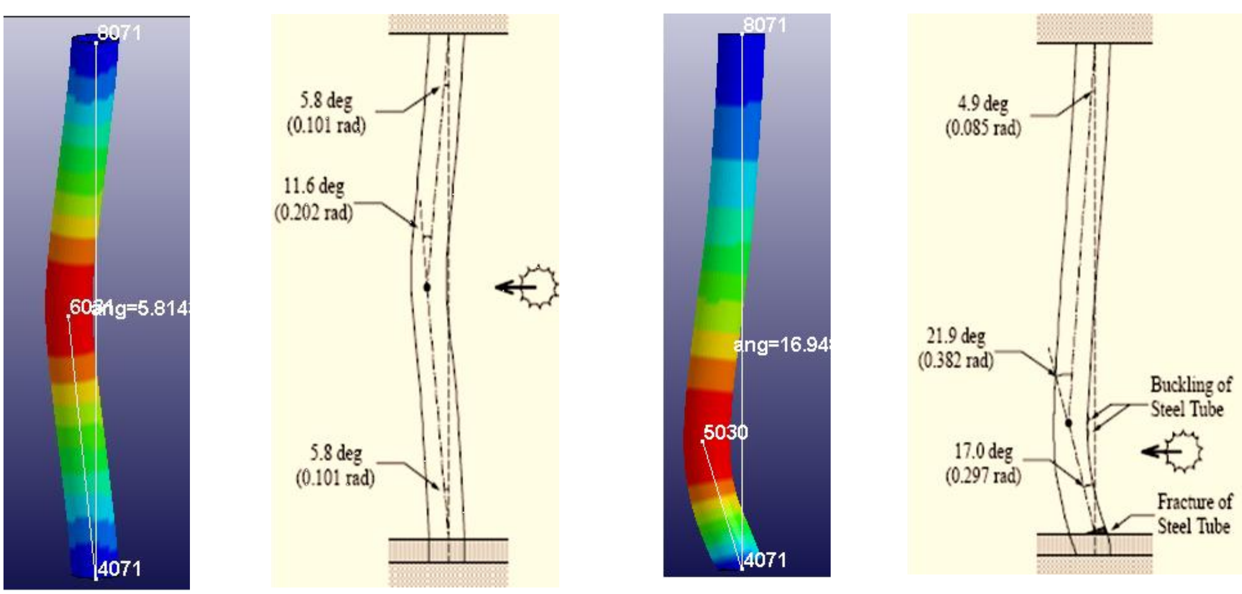

(a) (b)

Figure 4: (a) Plastic deformation in test 5, (b) Partial shell fracture in test 10

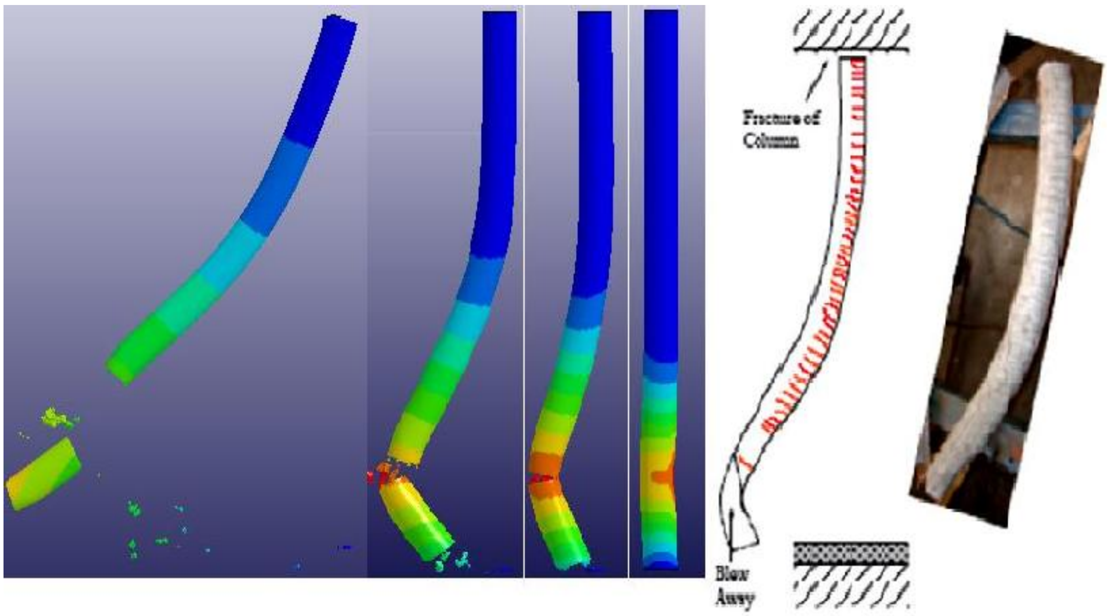

Figure 5: Fracture of the specimen in test 7.

5. PUSHOVER ANALYSIS OF CFDSTS

Pushover analysis are performed on the specimens derived from CFST64 using elastoplastic assumption for the steel with the yield stress and modulus elasticity set as measured in the experimental work by Marson and Bruneau. Those pushover analyses were used to determine the parameters affecting the strength and ductility of CFDST and to guide the selections of the specimens for blast analysis considering both pushover and blast analysis can bring a section to a critical deformed state. The implicit-explicit switch in LS-DYNA is used here to avoid convergence problem in the buckling-post buckling analysis of the sections studied. Figure 6 below show a comparison between the CFDSTs specimens and CFST64.

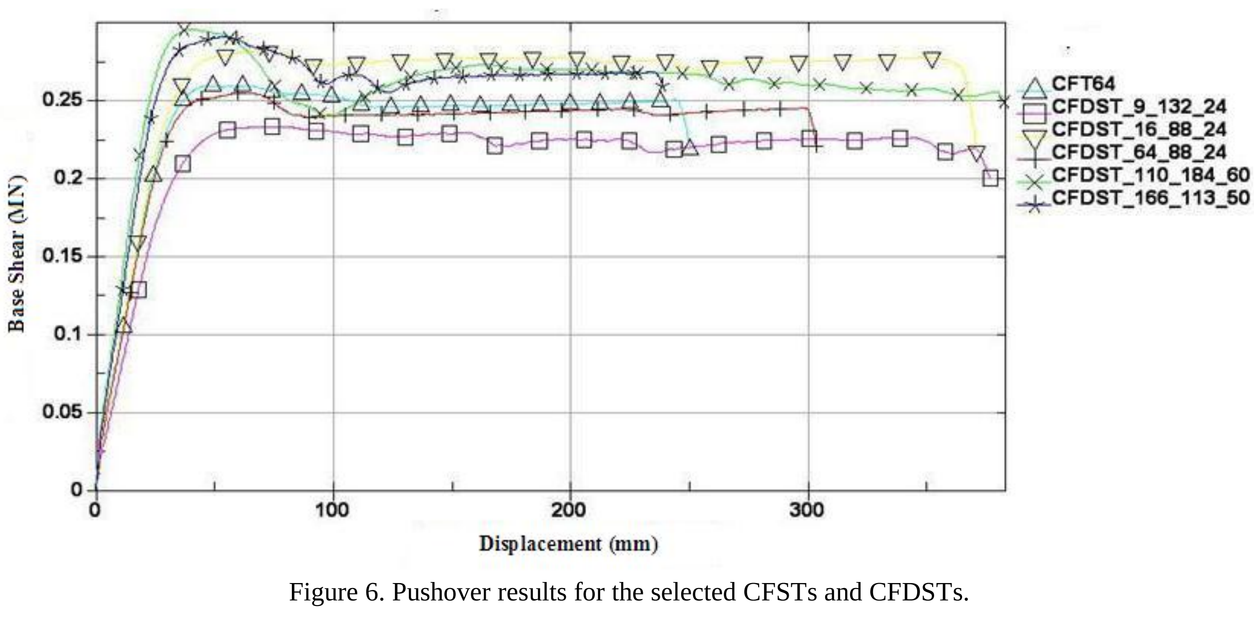

Figure 6. Pushover results for the selected CFSTs and CFDSTs.

From Figure 6 several conclusions for the optimal geometry of CFDST can be drawn. One is more compact inner and outer tubes result in sections less susceptible to post-peak buckling, more ductile and capable to maintain their ultimate strength over a longer yield plateau (see curve for CFDST16_88_24 and CFDST64_88_24). Another is that the compactness of the inner tube seems to control the ductility of the section overall. The pushover analysis also shows that, even for high depth-to-thickness ratios for the outside tubes, the CFDSTs are able to maintain their strength over a range of deformations comparable or even superior to that observed for the CFSTs. For large values of depth-to-thickness ratio a marked post peak drop is observed in the pushover curve which can be attributed to buckling of the outside tube, nevertheless the post-buckling behavior remains ductile afterwards. This suggests good confinement of the core by the steel tubes.

6. MULTIHAZARD FINITE ELEMENT ANALYSIS RESULTS OF CONCRETE-FILLED DOUBLE SKINNED TUBE

The results of the previous pushover analysis guided the selection of the CFDSTs shown on Table 4 for blast analysis and the selection of a candidate CFDST for cyclic pushover (CFDST16_88_24). So sections with low compactness ratios (less than the AISC limit of $0.15E/f_y$ for hollow steel tube, where E is the modulus of elasticity of the tube) are chosen, which incidentally keeps the void ratio to reasonable levels (less than 40%).

Under cyclic load, the CFDST candidate analysis conducted with LS-DYNA implicit yields comparable hysteresis behavior to that observed for CFST64 as shown on Figure 7 below. The ranges for both strength and displacement are similar. The CFDST specimen shows ductile post peak behavior with slow strength degradation which would be beneficial in resisting earthquake loading for a pier element with a CFDST cross section.

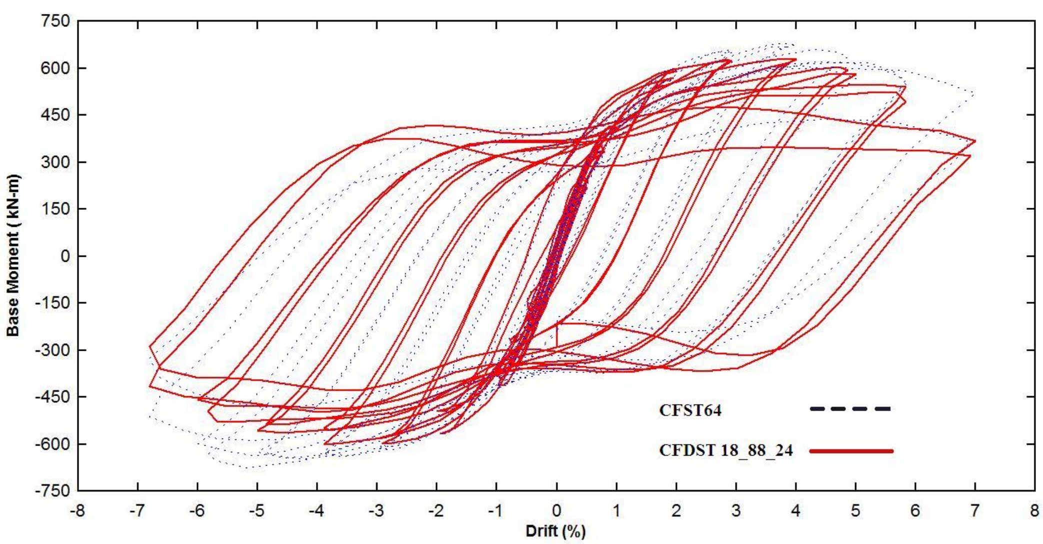

Figure 7. Hysteresis loops for cyclic analysis of CFDST_18_88_24

Analysis for blast load reveal that for the same scaled distances the CFDSTs fare better than the corresponding CFSTs. Reductions in displacement as high as 25% are achieved which corroborates the initial findings of the pushover analysis that, using the same amount of material, CFDSTs can be made at least as strong and ductile as CFSTs. Figure 8 shows comparison of the displacement histories of both types of section for tests 5 and 10. The actual results from the experiments are shown within the figure for comparison purpose. Figures 9 a) and b) show two different views at maximum deformation for each CFDST specimen; one of those views outlines both the core and the tubes. In Figure 9 b) No failure is visible for the CFDST which further demonstrates better performance compared to the corresponding CFST of test 10.

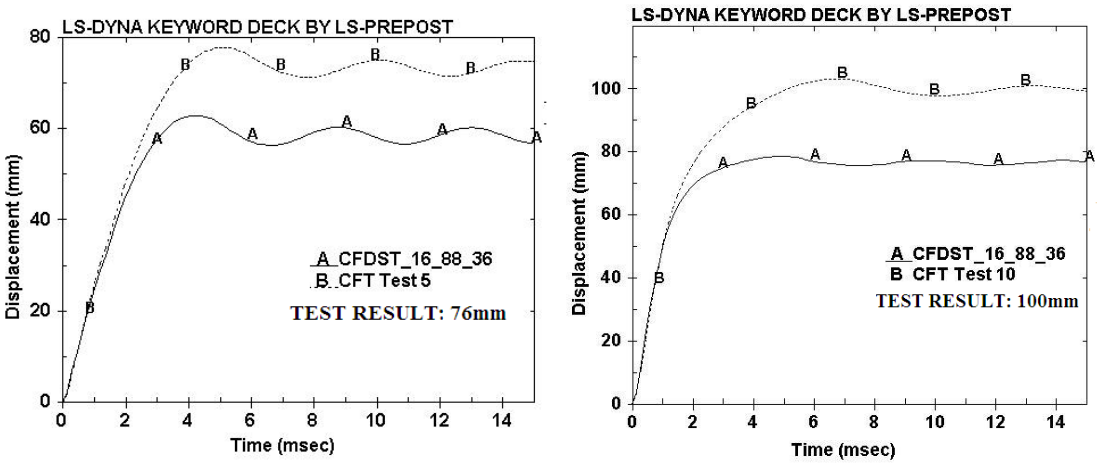

Figure 8. Comparison of displacement histories for CFST and CFDSTs for tests 5 and 10

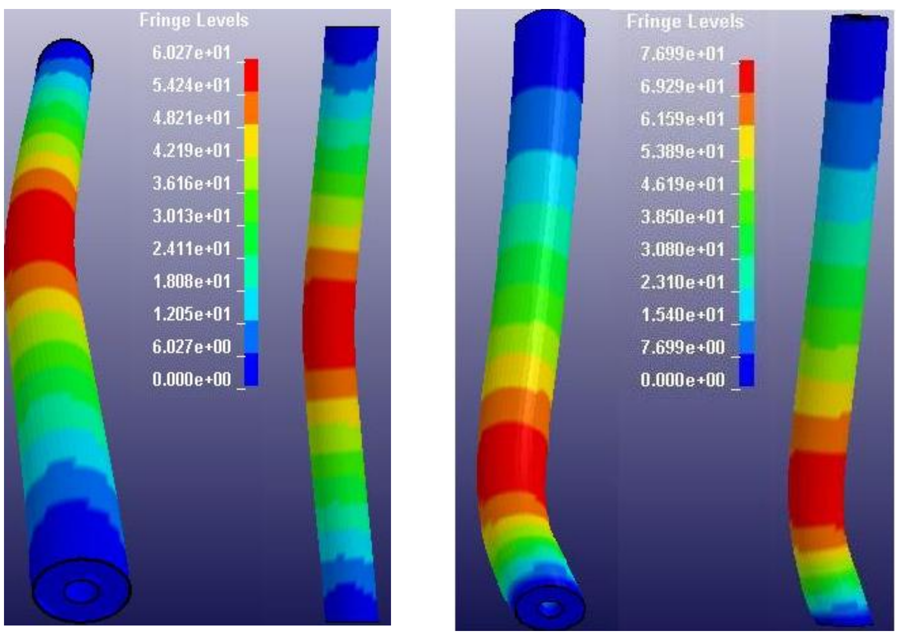

(a) (b)

Figure 9. Perspective and fringe plot views for (a) test 5 and (b) test 10

7. CONCLUSION

Advanced finite element analysis of concrete-filled tubes conducted with LS-DYNA show acceptable correlations with experimental results obtained for CFSTs under seismic and blast loading and predicts rather good performance for CFDSTs in the same conditions. However, further refinement of the finite element analysis under seismic loading of both sections might be needed to improve correlation with tests data with respect to pinching of the hysteretic curves.

In general, CFDSTs emulate CFSTs in terms of capacity to dissipate energy and, similarly, exhibits ductile behavior under load. CFDSTs can presumably reach higher deformation limit than CFSTs, however this needs to be experimentally validated to come up with safe limits for seismic and blast analysis.

8. ACKNOWLEDGMENTS

This research was supported in part by the Federal Highway Administration under contract number DTFH61-07-C-00020 to the Multidisciplinary Center for Earthquake Engineering Research. However, any opinions, findings, conclusions and recommendations presented in this paper are those of the authors and do not necessarily reflect the views of the sponsors.

9. REFERENCES

American Petroleum Institute (API). 1989. *Draft Recommended Practice for Planning, Designing and Constructing Fixed Offshore Platforms- Load and Resistance Factor Design*, API, RP2A-LRFD, Washington, D.C.

Fujikura, S., Bruneau, M., and Lopez-Garcia, D. 2007. *Experimental Investigation of Blast Performance of Seismically Resistant Concrete-Filled Steel Tube Bridge Piers*, Technical Report MCEER-07-0005, MCEER, University at Buffalo, Buffalo, NY.

Huang, Y., and Mahin, S.A. 2008. A Cyclic Damaged Plasticity Model: Implementation and Applications. *10th International LS-DYNA User's Conference*, Dearborn, Michigan, 14p. paper in conference proceedings.

Lin M.L. and Tsai K. C. 2001. Behavior of double-skinned composite steel tubular columns subjected to combined Axial and flexural loads. *First International Conference on Steel and Composite Structures*, Pusan, Korea, 8 p in proceedings

LSTC (2007). *LS-DYNA Keywords User's Manual*. Livermore Software Technology Corporation. Livermore, CA.

Malvar, J. L. and Simons, D. 1996. *Concrete Material Modeling in Explicit Computations*, Karagozian and Case. Glendale, CA.

Marson J. and Bruneau, M. 2000. *Cyclic Testing of Concrete-Filled Circular Steel Tube Brifge Columns Having Encased Fixed Base Detail*, Department of Civil Engineering, University of Ottawa, Ontario, Canada.

Montague, P. 1975. A Simple Composite Construction for Cylindrical Shells Subjected to External Pressure. *Journal of Mechanical Engineering Science*, 17 (2): 105-113.

Rust, W., and Schweizerhof, K. 2003. Finite Element Limit Load Analysis of Thin-Walled Structures by ANSYS (Implicit), LS-DYNA (Explicit) and in Combination. *Thin-Walled Structures*, 41 (2-3): 227-244.

Shakir-Khalil, H. 1991. Composite Columns of Double-Skinned Shells *Journal of Constructional Steel Research*, 19 (1991) : 133-152.

Tao, Z. et al. 2003. Behaviour of concrete-filled Double Skin (CHS inner and CHS outer) Steel Tubular Stub Columns and Beam-Columns. *Journal of Constructional Steel Research*, 60 (2003) : 1129-1158.

Wei S. et al. , 1995. Performance of New Sandwich Tube Under Axial Loading. *Journal of Structural Engineering*, 121 (12): 1814-1821.

.